X-932-74-358
PREPRINT

NASA TM X- 70857

SIMULATION OF A LUNAR GRADIOMETER MISSION

(NASA-TM-X-70857) SIMULATION OF A LUNAR GRADIOMETER MISSION (NASA) 26 p HC $3.75 CSCL 22A
N75-19327
Unclas
G3/15 14152

P. ARGENTIERO
R. GARZA-ROBLES

DECEMBER 1974

GSFC
GODDARD SPACE FLIGHT CENTER
GREENBELT, MARYLAND

For information concerning availability
of this document contact:

Technical Information Division, Code 250
Goddard Space Flight Center
Greenbelt, Maryland 20771

(Telephone 301-982-4488)

X-932-74-358

SIMULATION OF A LUNAR GRADIOMETER MISSION

P. Argentiero
R. Garza-Robles

December 1974

GODDARD SPACE FLIGHT CENTER
Greenbelt, Maryland

SIMULATION OF A LUNAR GRADIOMETER MISSION

P. Argentiero
R. Garza-Robles

ABSTRACT

A Lunar Gradiometer mission involves the mounting of a gradiometer on a satellite which is in a low, polar, and circular lunar orbit. This paper presents the results of a numerical simulation of the mission. It is shown that if the satellite is in a 50 km orbit, 1° and 2° gravity anomalies may be estimated with accuracies of 12 mgal and 1 mgal respectively. At a 100 km altitude, 2° gravity anomalies can be estimated with an accuracy of 12 mgal. These results assume a rotating type gradiometer with a .1E accuracy. The results can be readily scaled to reflect another accuracy level.

CONTENTS

ILLUSTRATIONS

SIMULATION OF A LUNAR GRADIOMETER MISSION

INTRODUCTION

For the purpose of estimating the lunar gravity field, the output of a gradiometer has advantages over satellite perturbation data. The gradiometer, since it can measure second derivatives of the lunarpotential field, will be sensitive to the density variations of the Moon's outer crust which are the source of the significant high frequency components of the lunarpotential field. These high frequency effects tend to be smoothed out in satellite perturbation data.

Regardless of what data type one employs there are difficulties in using standard parameter estimation techniques to determine a global and detailed lunar gravity field. The essence of these difficulties is that a large number of parameters must be estimated. For instance, if features of the lunar potential as small as 2° are to be recovered and if the standard spherical harmonic expansion of the lunarpotential field is used as a parameterization, a full set of coefficients to degree and order 90 is required. This implies the estimation of over 8000 parameters. In general it is not possible to simultaneously estimate such large parameter sets. In practice, in order to use standard estimation techniques to recover lunarpotential fine structure from gradiometer data, it will be necessary to adjust small subsets of parameters while constraining other parameters to a priori values. But unless the parameterization exhibits a certain orthogonality property in the data set the effect is that the uncertainties in the unadjusted terms will badly corrupt the estimates of the adjusted terms. If spherical harmonic coefficients are utilized the estimation problem can be decomposed into estimation problems of smaller dimensionality only if the gradiometer data set is globally distributed. This implies a heavy computational load. A parameterization of the lunarpotential field is desired in which the individual parameters exhibit a localized observability pattern in gradiometer data. With such a parameterization it would be possible to accurately estimate small subsets of parameters by processing localized blocks of gradiometer data. The mean free air gravity anomaly - Stokes' function parameterization of a gravity field [1] has been shown to possess a measure of orthogonality in local blocks of altimeter data [2]. In [3] the observability of gravity anomalies in gradiometer data was shown but the orthogonality property was assumed rather than demonstrated. To be realistic one must recognize that the orthogonality is not perfect and that only the estimates of gravity anomalies which are a sufficient distance from unadjusted gravity anomalies will be of value. This implies that gravity anomalies should be estimated in blocks with the estimates of anomalies in a sufficiently small inner core accepted as valid and the rest rejected due to aliasing. To obtain an intelligent estimation strategy for estimating lunar gravity anomalies from gradiometer data it is necessary to determine for a given data block size the relationship between the accuracy with which a given anomaly is estimated and its distance from the nearest unadjusted anomaly.

In this report lunar gradiometer missions at 50 km and 100 km altitude are simulated and optimal data block and estimation block sizes for determining 1° and 2° lunar gravity anomalies are obtained by means of covariance analysis. A rotating type gradiometer as described in [4] is assumed mounted on a lunar polar satellite and to have an accuracy of .1 E, (1 E = 10^{-9} gal/cm). The results can be readily scaled to reflect any other accuracy level.

ORTHOGONALITY PROPERTIES OF GRAVITY ANOMALIES IN GRADIOMETER DATA

The rotating gradiometer is an instrument which senses gravity gradients in a given plane. If the instrument is on board a satellite we take that plane to be the orbital plane of the satellite. Define a local satellite centered coordinate system (I_1, I_2, I_3) where the I_1 unit vector is pointing northward, the I_2 unit vector is pointing eastward, and the I_3 unit vector is perpendicular to the plane spaned by I_1 and I_2 and is directed outward from the moon. If the satellite on which the rotating gradiometer is mounted is in a polar orbit, the sensing plane of the instrument always coincides with the plane spanned by the I_2 and I_3 unit vectors. This assumption considerably simplifies the following mathematical development. The lunarpotential field can be represented as

$$W = U + T \tag{1}$$

where U is a reference lunarpotential generally defined by a low degree and order spherical harmonic expansion of a nominal field and T is the so-called anomalous potential. The anomalous potential represents the high frequency part of the field and we are primarily interested in the portion of the gradiometer output which is due to T. Assuming that the satellite is in a polar orbit, the additive component of the rotating gradiometer signal amplitude which is due to the anomalous potential T is

$$\mathrm{AMP} = \left(\left[\frac{\partial^2 T(r,\phi,\lambda)}{\partial r^2} - \frac{1}{r^2}\frac{\partial^2 T(r,\phi,\lambda)}{\partial \phi^2}\right]^2 + 4\left[\frac{1}{r}\frac{\partial^2 T(r,\phi,\lambda)}{\partial r \partial \phi}\right]^2\right)^{1/2} \tag{2}$$

where r, ϕ, and λ have the usual spherical coordinate interpretations and where the derivatives are evaluated at the satellite position [3].

The anomalous potential T at any point above the surface of the moon can be expressed by means of the discrete form of Stokes' formula as

$$T(r, \phi, \lambda) = \sum_i \delta g_i(\phi_i', \lambda_i')\, S(r, \phi, \lambda, \phi_i', \lambda_i') \cos(\phi_i')\, \Delta\phi_i'\, \Delta\lambda_i' \tag{3}$$

where $\delta g_i\ (\phi_i', \lambda_i')$ is a mean gravity anomaly over a block centered at latitude ϕ_i'; and longitude λ_i' and referenced to a equipotential surface defined by the nominal field U. The expression $\cos(\phi_i')\, \Delta\phi_i'\, \Delta\lambda_i'$ represents the area of the block on which the i^{th} gravity anomaly is defined and $S(r, \phi, \lambda, \phi_i', \lambda_i')$ is Stokes' function given in [3] by

$$S(r, \phi, \lambda, \phi', \lambda') = t\left[\frac{2}{D} + 1 - 3D - t\cos(\psi)\left(5 + 3\,\ell n\left[\frac{1 + t\cos(\psi) + D}{2}\right]\right)\right] \tag{4}$$

where

$$\psi = \cos^{-1} [\sin(\phi) \sin(\phi') + \cos(\phi) \cos(\phi') \cos(\lambda' - \lambda)]$$

$$t = \frac{R}{r}$$

$$D = (1 - 2t\cos(\psi) + t^2)^{1/2}$$

where R is the mean radius of the moon. The functional relationship between the anomalous part of the gradiometer output and a globally distributed set of gravity anomalies is obtained from Equations 2 and 3 as

$$\mathrm{AMP} = \sum_i \left(\left[\frac{\partial^2 S(r,\phi,\lambda,\phi_i',\lambda_i')}{\partial r^2} - \frac{1}{r^2} \frac{\partial^2 S(r,\phi,\lambda,\phi_i',\lambda_i')}{\partial \phi^2} \right]^2 + 4 \left[\frac{1}{r} \frac{\partial^2 S(r,\phi,\lambda,\phi_i',\lambda_i')}{\partial r \partial \phi} \right]^2 \right)^{1/2} \cos(\phi_i') \Delta\phi_i' \Delta\lambda_i' \delta g(\phi_i',\lambda_i') \quad (5)$$

Equation 5 shows that if the discrete form of Stokes' formula is valid, the gradiometer output is a linear function of a global distribution of gravity anomalies. Hence standard parameter estimation techniques should be applicable to the problem of determining gravity anomalies from gradiometer data. To see how these techniques are applied it is useful to employ matrix notation. Let $\tilde{y}$ be a vector of the anomalous components of gradiometer readings. Assume that the i^{th} component of $\tilde{y}$ is the anomalous gradiometer reading obtained when the satellite's position is given in spherical coordinates as (r_i, ϕ_i, λ_i). Let $\tilde{g}$ be a vector of numerical values of a global set of gravity anomalies. The j^{th} component of $\tilde{g}$ is the numerical value of the gravity anomaly centered at latitude ϕ_j' and longitude λ_j'. The functional relationship between $\tilde{y}$ and $\tilde{g}$ is expressed as

$$\tilde{y} = A\tilde{g} \quad (6)$$

where A is a matrix the number of whose rows is the number of observations and the number of whose columns is the number of gravity anomalies. The element in the i^{th} row and j^{th} column of A is

$$A(I,J) = \left(\left[\frac{\partial^2 S(r,\phi_i,\lambda_i,\phi_j',\lambda_j')}{\partial r_i^2} - \frac{1}{r_i^2} \frac{\partial^2 S(r_i,\phi_i,\lambda_i,\phi_j',\lambda_j')}{\partial \phi_i^2} \right]^2 + 4 \left[\frac{1}{r_i} \frac{\partial^2 S(r_i,\phi_i,\lambda_i,\phi_j',\lambda_j')}{\partial r_i \, \partial \phi_i} \right]^2 \right)^{1/2} \cos(\phi_j') \Delta\phi_j' \Delta\lambda_j' \quad (7)$$

Equation 7 provides a linear equation of condition and in a standard minimum variance fashion $\tilde{g}$ could be estimated from observations of $\tilde{y}$. In order for Equation 7 to be correct (correct, that is, assuming that the approximations inherent in the discrete form of Stokes' formula are valid) the gravity anomalies in the array $\tilde{g}$ must cover the moon's surface. Computational considerations constrain us to choose a region such that the number of gravity anomalies to be estimated does not exceed a few hundred. In effect gravity anomalies outside of this region are assumed to be zero. To see precisely what happens when this assumption is made postulate the $\tilde{g}$ array of Equation 6 to be defined over the globe, and write

$$\tilde{g} = \begin{bmatrix} \tilde{g}_1 \\ \hline \tilde{g}_2 \end{bmatrix}$$

where

$\tilde{g}_1$ = gravity anomalies to be adjusted in a standard minimum variance filter and

$\tilde{g}_2$ = gravity anomalies assumed to be zero and thus left unadjusted by the minimum variance filter.

Then Equation 6 can be written

$$\tilde{y} = A_1 \tilde{g}_1 + A_2 \tilde{g}_2 \tag{8}$$

where A_1 and A_2 are respectively the variational matrices of $\tilde{y}$ with respect to $\tilde{g}_1$ and $\tilde{g}_2$.

The gradiometer output provides direct observations y of $\tilde{y}$ with statistics

$$y = \tilde{y} + \nu,\ E(\nu) = \bar{0},\ E(\nu \nu^T) = Q \tag{9}$$

The gravity anomalies $\tilde{g}_2$ for computational reasons are assumed to be zero but the actual values of gravity anomalies in the region of the sphere which is ignored have a certain distribution about zero. We assume

$$E(\tilde{g}_2) = \bar{0},\ E(\tilde{g}_2 \tilde{g}_2^T) = P_2 \tag{10}$$

When the values of $\tilde{g}_2$ are assumed to be zero the minimum variance estimate of $\tilde{g}_1$ becomes

$$\hat{g}_1 = (A_1^T Q^{-1} A_1)^{-1} A_1^T Q^{-1} y \tag{11}$$

Define the covariance matrix of the estimator given by Equation 11 as

$$P = E([\hat{g}_1 - \tilde{g}_1]\ [\hat{g}_1 - \tilde{g}_1]^T) \tag{12}$$

From Equations 9, 10, and 11 we obtain

$$\hat{g}_1 - \tilde{g}_1 = (A_1^T Q^{-1} A_1)^{-1} (-A_1^T Q^{-1} A_2 \tilde{g}_2 + A_1^T Q^{-1} \nu) \tag{13}$$

Equation 13 yields

$$P = (A_1^T Q^{-1} A_1)^{-1} + (A_1^T Q^{-1} A_1)^{-1} A_1^T Q^{-1} A_2 P_2 A_2^T Q^{-1} A_1 (A_1^T Q^{-1} A_1)^{-1} \tag{14}$$

Assume that the data noise is uncorrelated and that each data point has the same variance. Then

$$Q = I\sigma_0^2 \tag{15}$$

where I is the identity matrix and σ_0^2 is the common variance of the data. On the assumption that the values of the unadjusted gravity anomalies are independently distributed, the covariance matrix P_2 of $\tilde{g}_2$ can be written as

$$P_2 = \begin{bmatrix} \sigma_1^2 & & & \\ & \sigma_2^2 & & 0 \\ & 0 & \ddots & \\ & & & \sigma_{n_2}^2 \end{bmatrix} \tag{16}$$

where n_2 is the number of unadjusted gravity anomalies and σ_i^2 is the second moment about zero of the i^{th} unadjusted gravity anomaly. Also define a matrix K as

$$K = (A_1^T Q^{-1} A_1)^{-1} A_1^T Q^{-1} A_2 \tag{17}$$

If n_1 is the number of adjusted parameters, then K is of dimension n_1 by n_2. With these assumptions Equation 14 yields the following expression for the variance of the i^{th} adjusted gravity anomaly

$$P(I, I) = \sum_{j=0}^{n_2} (\beta_{i,j}\, \sigma_j)^2 \tag{18}$$

where $\beta_{i,0}^2$ is the i^{th} diagonal element of the matrix $(A_1^T A_1)^{-1}$ and

$$\beta_{i,j} = K(I, j), j \geqslant 1 \tag{19}$$

Define the error sensitivity matrix as

$$S = \left\{\beta_{i,j}\right\}, i = 1, 2, ..., n_1, J = 0, 1, 2, ..., n_2 \tag{20}$$

And finally define the alias matrix as

$$L = S\overline{\sigma} \tag{21}$$

where

$$\overline{\sigma} = \begin{bmatrix} \sigma_0 & & & & 0 \\ & \sigma_1 & & & \\ & & \sigma_2 & & \\ & 0 & & \cdot & \\ & & & & \cdot \\ & & & & \sigma_{n_2} \end{bmatrix} \tag{22}$$

The alias matrix reveals much of the probability structure of the estimation procedure. From Equations 18, 20, 21 and 22 it can be seen that the standard deviation of the i^{th} adjusted gravity anomaly is the root sum square of the terms in the i^{th} row of the alias matrix. The elements in the first column of the alias matrix represent the R.S.S. contribution to the standard deviation of each estimated parameter due to the data noise. The elements in the j^{th} column, $j \geq 2$ represent the R.S.S. contribution to the standard deviation of each estimated parameter due to the $j - 1^{st}$ unadjusted parameter. These terms are called <u>the aliasing contributions</u> to the uncertainty in the adjusted parameters due to the <u>uncertainty of the $j - 1^{st}$</u> unadjusted parameter. Notice that the aliasing contributions due to the j^{th} unadjusted parameter are proportional to the standard deviation of the j^{th} parameter.

DEFINITION

> In a given estimation process the i^{th} estimated parameter is said to be <u>orthogonal</u> with respect to the j^{th} unestimated parameter if the aliasing contribution to the i^{th} estimated parameter due to the uncertainty of the j^{th} unestimated parameter is zero. It will be seen that the relation is symetric in the sense that if one parameter is orthogonal with respect to another and if they are interchanged within the adjusted and unadjusted modes, they are again orthogonal.

To see the implications of the orthogonality relationship we need a more revealing representation of the aliasing terms. Notice that the first term on the right side of Equation 14 is the covariance matrix of the estimation process under the assumption that the unadjusted parameters are perfectly known. This covariance matrix gives the uncertainty of the estimates due only to the data noise. Define the so-called "noise only" covariance matrix as

$$P = (A_1^T Q^{-1} A_1)^{-1} \tag{23}$$

Next observe that the elements in the i^{th} row and j^{th} column of respectively A_1 and A_2 are the partial derivatives of the i^{th} data point with respect to the j^{th} adjusted parameter and the partial derivative of the i^{th} data point with respect to the j^{th} unadjusted parameter. The aliasing contribution to the i^{th} adjusted parameter due to the j^{th} unadjusted parameter can be written as

$$L(I, j+1) = \sum_{k=1}^{n_1} \bar{P}(I, k) \sum_{\ell=1}^{m} \frac{\partial \tilde{y}(\ell)}{\partial \tilde{g}_1(k)} Q^{-1}(\ell, \ell) \frac{\partial \tilde{y}(\ell)}{\partial \tilde{g}_2(j)} \tag{24}$$

where m is the number of data points. If the estimates of the adjusted parameters are relatively uncorrelated in the noise only covariance matrix, Equation 24 can be approximated by

$$L(I, j+1) = \bar{P}(I, I) \sum_{\ell=1}^{m} \frac{\partial \tilde{y}(\ell)}{\partial \tilde{g}_1(I)} Q^{-1}(\ell, \ell) \frac{\partial \tilde{y}(\ell)}{\partial \tilde{g}_2(j)} \tag{25}$$

From Equation 25 we see that the aliasing contribution is symetric in its arguments and this implies the symetry of the orthogonality relationship.

A sufficient condition for the left side of Equation 25 to approximate zero is for the observability patterns of $\tilde{g}_1(I)$ and $\tilde{g}_2(j)$ in the data to be virtually nonoverlapping. Figures 1 and 2 demonstrate that the perturbation of a gradiometer observation due to a 1 mgal perturbation of a gravity anomaly rapidly attenuates with increasing spherical radius. Hence if the grids on which $\tilde{g}_1(I)$ and $\tilde{g}_2(j)$ are defined are sufficiently separated, the orthogonality relationship would be effectively satisfied and the estimate of $\tilde{g}_1(I)$ would experience no aliasing from the uncertainty of $\tilde{g}_2(j)$. Conversely, if the grid on which $\tilde{g}_1(I)$ was defined were in close proximity to grids whose gravity anomalies were unadjusted, one would expect serious aliasing of the resultant estimate.

It should be clear then, that if the gravity anomalies are estimated in a block the outer layers of the block contain gravity anomalies whose estimates will be badly aliased by the adjacent unadjusted parameters. It will be necessary to discard these estimates. But the gravity anomalies in a sufficiently small inner core of the block may be adequately separated from the unadjusted parameters to be effectively orthogonal with respect to them. The estimates of these terms

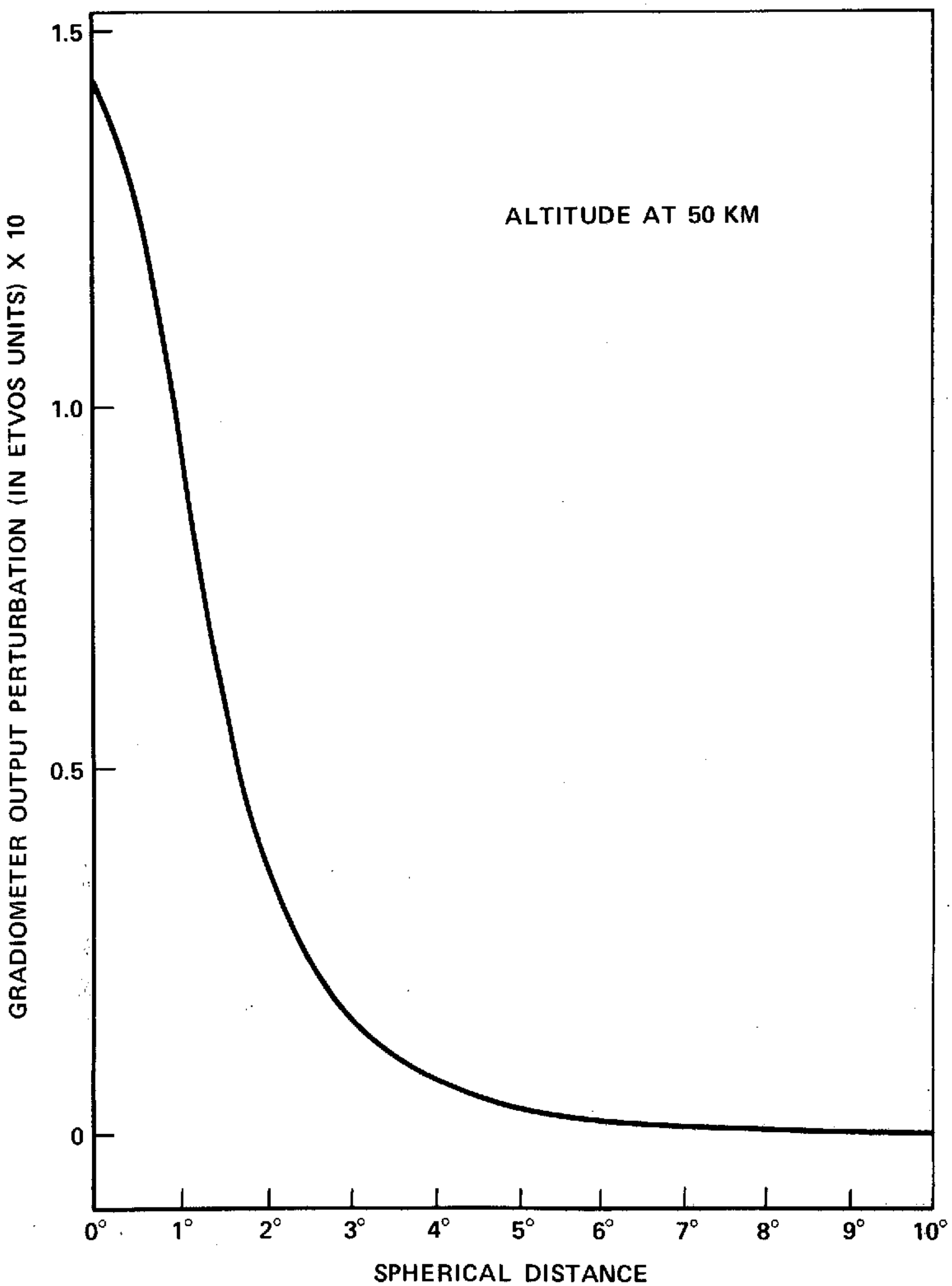

Figure 1. Gradiometer Output Perturbation Due to 1 mgal Perturbation of 2° Lunar Gravity Anomaly

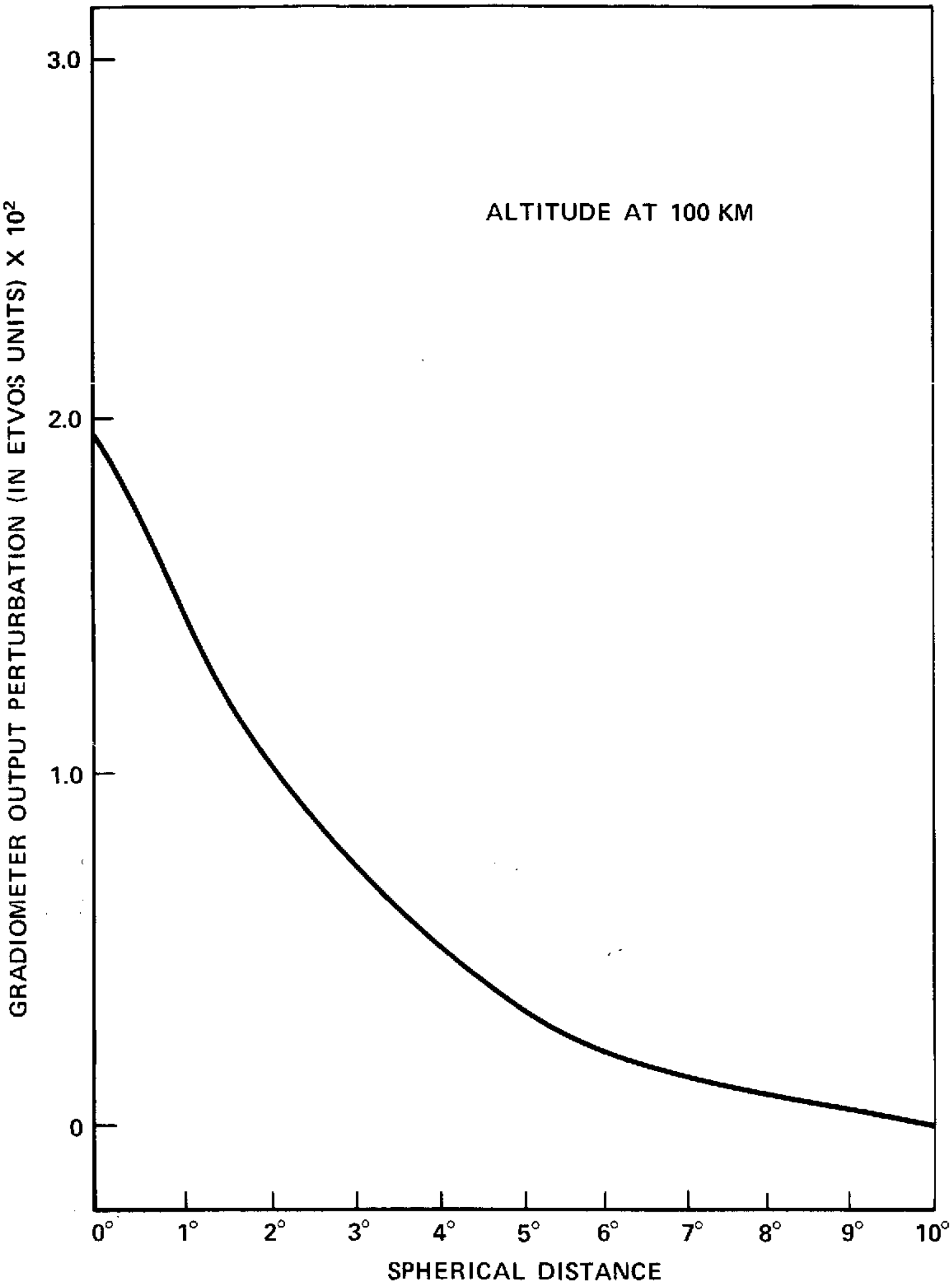

Figure 2. Gradiometer Output Perturbation Due to 1 mgal Perturbation of 2° Lunar Gravity Anomaly

presumably will be of sufficient accuracy that they can be accepted. In effect, for every block of gravity anomalies that we intend to estimate it will be necessary to construct of "buffer zone" several layers deep of gravity anomalies which surround the block. The new and larger block of gravity anomalies must be simultaneously estimated and then the estimates of gravity anomalies in the buffer zone must be rejected due to aliasing. To design an intelligent data processing procedure for a lunar gradiometer mission it is necessary to know the relationship between the depth of the buffer zone and the accuracy of the estimation procedure. This relationship will vary with grid size, data block size, and satellite altitude. The most efficient way to study the relationship is to utilize covariance analysis techniques to generate alias matrices for several situations and to attempt generalizations from the results. This is accomplished in the next section.

RESULTS

Assuming a satellite altitude of approximately 100 km and that a gradiometer reading is obtained every 15 seconds, a dense globally distributed set approximately 86,000 gradiometer measurements are obtained within 15 days. In the low latitudes the sublunar points of the satellite at the measurement times form a grid on the moon of 75 degrees latitude by one degree longitude. All our simulations rely on this assumption concerning the data distribution. In doing so we eliminate the dynamical aspect of the problem and thus the aliasing effect of orbit determination and attitude determination errors are not included in our results.

As mentioned in the introduction the reason for employing gravity anomalies to describe lunarpotential fine structure is the possibility of successfully estimating local blocks of gravity anomalies in local blocks of gradiometer data. To investigate this possibility we focus attention on the estimation accuracy of a single gravity anomaly as a function of the number of adjacent gravity anomalies which are simultaneously adjusted and the quantity of data which is used in the estimation. We define the estimation block to be a block of gravity anomalies centered at the gravity anomaly in question and square in the sense that the block subtends the same number of degrees longitude as latitude. We assume that all the gravity anomalies in the estimation block are simultaneously adjusted in a given estimation procedure. As we have defined it, estimation blocks can only be incremented by integral numbers of twice the gravity anomaly block size. For 2° gravity anomalies, for instance, possible estimation block sizes are 2°, 6°, 9°, 10°, 14°, etc.

The data block is defined as a gradiometer data set which was obtained when the sublunar points of the satellite were within a square region of the lunar surface centered at the gravity anomaly in question. For a given estimation block size the accuracy of a gravity anomaly estimate is not necessarily a monotone function of the data block size. This may at first be puzzling since in general one expects more data to yield better estimates. An explanation can be obtained by noticing that for a given estimation block the covariance matrix of the set of estimated gravity anomalies is given by Equation 14 as the sum of a matrix which is dependent only on data uncertainty and a matrix which represents the aliasing effects from the unadjusted parameters. With increasing data blocks the elements of the first matrix must decrease but in general the elements of the matrix which conveys the aliasing effects will increase. This effect can be shown graphically by means of so-called aliasing maps. To obtain the aliasing maps of Figures 3 and 4 we simulate in a covariance mode a situation in which we describe lunarpotential fine structure by means of 2° by 2° gravity anomalies and we assume gradiometer data with an accuracy of .1E. In Figure 3 we mapped

0	0	0	0	0	0	0	0	0	0	0	0	0	0	0	0	0	0	0	0
0	0	0	0	0	0	0	0	0	0	0	0	0	0	0	0	0	0	0	0
0	0	0	0	0	0	0	0	0	0	0	0	0	0	0	0	0	0	0	0
0	0	0	0	0	0	0	0	0	0	0	0	0	0	0	0	0	0	0	0
0	0	0	0	0	0	0	0	0	0	0	0	0	0	0	0	0	0	0	0
0	0	0	0	0	0	0	0	0	0	0	0	0	0	0	0	0	0	0	0
0	0	0	0	0	0	0	0	0	0	0	0	0	0	0	0	0	0	0	0
0	0	0	0	0	0	0	0	0	0	0	0	0	0	0	0	0	0	0	0
0	0	0	0	0	0	0	0	1	3	3	3	1	0	0	0	0	0	0	0
0	0	0	0	0	0	0	1	6	19	30	18	6	1	0	0	0	0	0	0
0	0	0	0	0	0	0	3	9	40		39	9	3	0	0	0	0	0	0
0	0	0	0	0	0	0	1	6	16	25	16	6	1	0	0	0	0	0	0
0	0	0	0	0	0	0	0	1	1	3	1	1	0	0	0	0	0	0	0
0	0	0	0	0	0	0	0	0	0	0	0	0	0	0	0	0	0	0	0
0	0	0	0	0	0	0	0	0	0	0	0	0	0	0	0	0	0	0	0
0	0	0	0	0	0	0	0	0	0	0	0	0	0	0	0	0	0	0	0
0	0	0	0	0	0	0	0	0	0	0	0	0	0	0	0	0	0	0	0
0	0	0	0	0	0	0	0	0	0	0	0	0	0	0	0	0	0	0	0
0	0	0	0	0	0	0	0	0	0	0	0	0	0	0	0	0	0	0	0
0	0	0	0	0	0	0	0	0	0	0	0	0	0	0	0	0	0	0	0

5° DATA BLOCK
50 KM SATELLITE HEIGHT

Figure 3. Alias Map for 2° Gravity Anomalies

0	0	0	0	0	0	0	0	0	0	0	0	0	0	0	0	0	0	0	0
0	0	0	0	0	0	0	0	0	0	0	0	0	0	0	0	0	0	0	0
0	0	0	0	0	0	0	0	0	0	0	0	0	0	0	0	0	0	0	0
0	0	0	0	0	0	0	0	0	0	0	0	0	0	0	0	0	0	0	0
0	0	0	0	0	0	0	0	0	0	0	0	0	0	0	0	0	0	0	0
0	0	0	0	0	0	0	0	0	0	0	0	0	0	0	0	0	0	0	0
0	0	0	0	0	0	0	0	0	0	0	0	0	0	0	0	0	0	0	0
0	0	0	0	0	0	0	1	1	1	1	1	1	1	0	0	0	0	0	0
0	0	0	0	0	0	1	3	4	6	6	6	4	3	1	0	0	0	0	0
0	0	0	0	0	1	3	6	12	22	30	22	12	6	3	1	0	0	0	0
0	0	0	0	0	1	3	7	16	43		45	18	7	3	1	0	0	0	0
0	0	0	0	0	1	3	6	12	22	30	22	12	6	3	1	0	0	0	0
0	0	0	0	0	0	1	3	4	6	6	6	4	3	1	0	0	0	0	0
0	0	0	0	0	0	0	1	1	1	1	1	1	1	0	0	0	0	0	0
0	0	0	0	0	0	0	0	0	0	0	0	0	0	0	0	0	0	0	0
0	0	0	0	0	0	0	0	0	0	0	0	0	0	0	0	0	0	0	0
0	0	0	0	0	0	0	0	0	0	0	0	0	0	0	0	0	0	0	0
0	0	0	0	0	0	0	0	0	0	0	0	0	0	0	0	0	0	0	0
0	0	0	0	0	0	0	0	0	0	0	0	0	0	0	0	0	0	0	0
0	0	0	0	0	0	0	0	0	0	0	0	0	0	0	0	0	0	0	0

20° DATA BLOCK
50 KM SATELLITE HEIGHT

Figure 4. Alias Map for 2° Gravity Anomalies

the R.S.S. contribution in mgals to the uncertainty in the estimate of the gravity anomaly defined on the blank grid element in the middle of the graph when the adjacent gravity anomalies are assumed to be in an unadjusted mode and to have an a priori uncertainty of 75 mgals. The data block as represented by the shaded area of the graph is 5° on a side. The satellite altitude was 50 km. Notice that the aliasing contributions decrease with the distance between an unadjusted parameter and the estimated parameter thus demonstrating the inherent orthogonality properties of gravity anomalies in gradiometer data. In Figure 4 the data block size has been increased to 20° and the aliasing effect of adjacent unadjusted gravity anomalies is seen to be greater.

The choice of an intelligent data reduction strategy is obviously dependent on a knowledge of the relationship between estimation accuracy and the choice of data block size and estimation block size. A computer program was written which computes the right side of Equation 14 for any given data reduction technique. The program was used to investigate data reduction strategies. First an altitude for the satellite was chosen and a gradiometer data block centered on a chosen gravity anomaly was assumed. The data accuracy was assumed as .1E. A normal matrix for 400 gravity anomalies was formed. The chosen gravity anomaly and gravity anomalies in successive layers surrounding the chosen gravity anomaly were assumed to be in an adjusted mode and the rest were placed in an unadjusted mode with uncertainties about zero of 75 mgal. The right side of Equation 14 was computed and the resultant standard deviation in the estimate of the chosen gravity anomaly was recorded. The estimation block size was incremented by removing another layer of gravity anomalies from the unadjusted to the adjusted mode and repeating the process. Figures 5 and 6 display the relationship between estimates of 1° and 2° gravity anomalies and the choices of data block size and estimation block size when the satellite is at an altitude of 50 km. Figure 7 displays the information when the satellite is at 100 km.

The graphs show that for 2° gravity anomalies an intelligent compromise between computational load and accuracy is achieved when a data block size of 5° is employed and the buffer zone of rejected gravity anomaly estimates is at least two layers deep. The graphs show that when this strategy is followed and if the satellite is in a 50 km orbit, 2° gravity anomalies can be estimated with an accuracy of less than 1 mgal. For 1° gravity anomalies the best strategy utilizes a 10° data block size and a buffer zone of rejected gravity anomaly estimates five layers deep. With this strategy 1° gravity anomalies can be estimated to an accuracy of about 12 mgal. At an altitude of 100 km, 1° gravity anomalies cannot be effectively estimated. Figure 7 shows that 2° gravity anomalies can be estimated from a satellite height of 100 km to an accuracy of 12 mgal provided a 20° data block size is utilized and provided that a buffer zone of rejected gravity anomalies five layers deep is utilized.

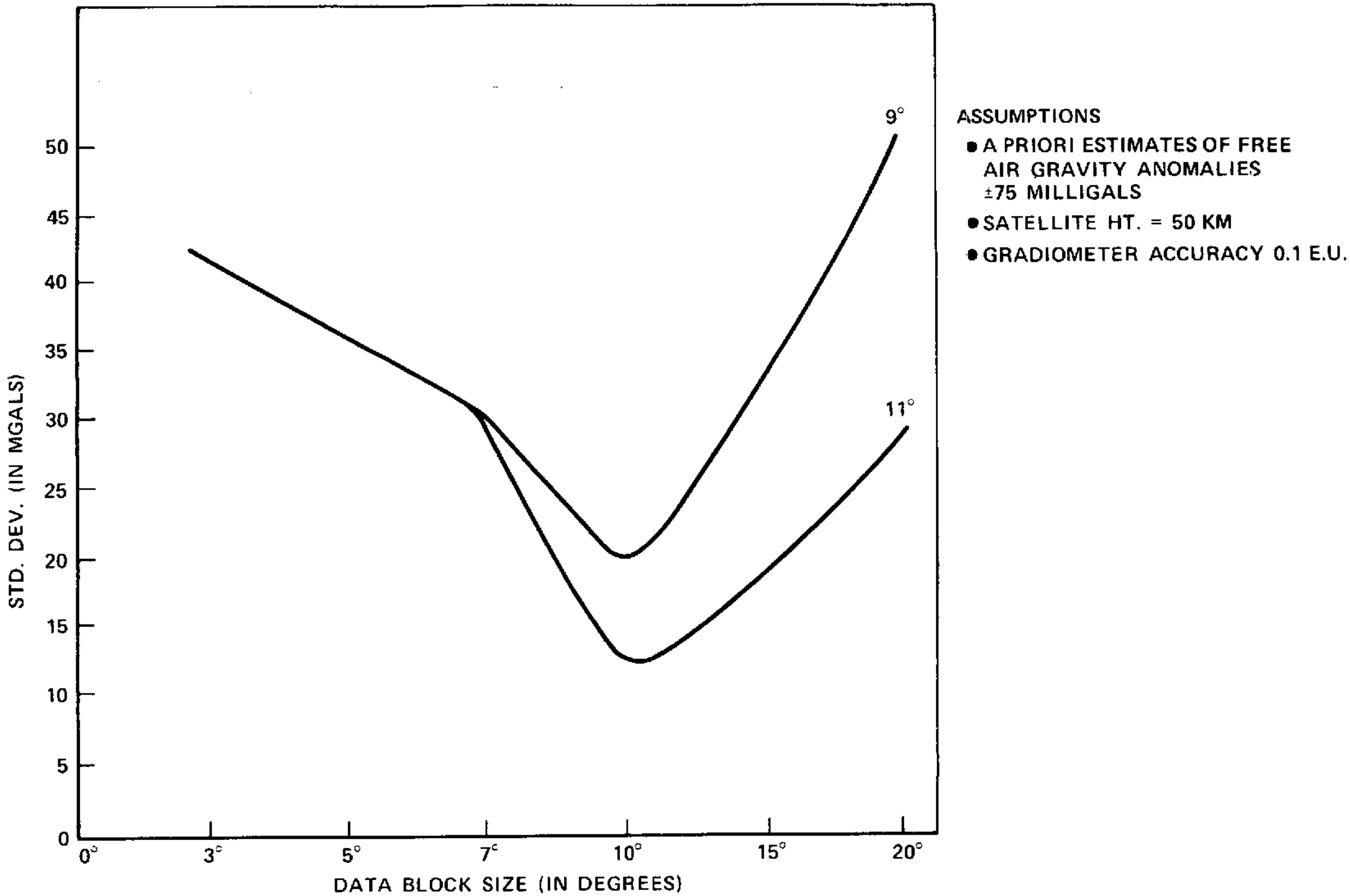

Figure 5. Accuracy of 1° by 1° Mean Free Air Gravity Anomaly Estimates vs. Data Block Size for Various Estimation Block Sizes

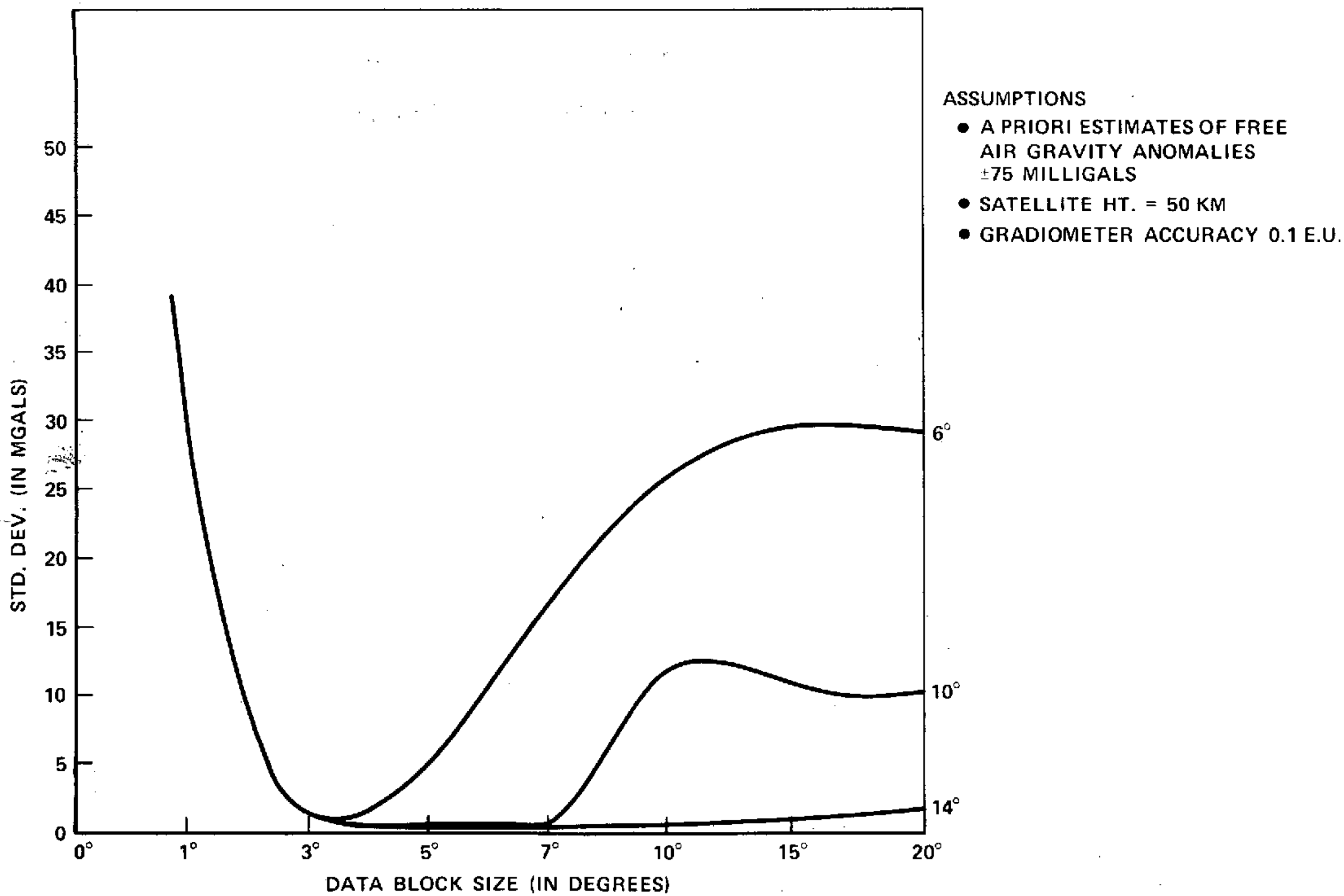

Figure 6. Accuracy of 2° by 2° Mean Free Air Gravity Anomaly Estimates vs. Data Block Size for Various Estimation Block Sizes

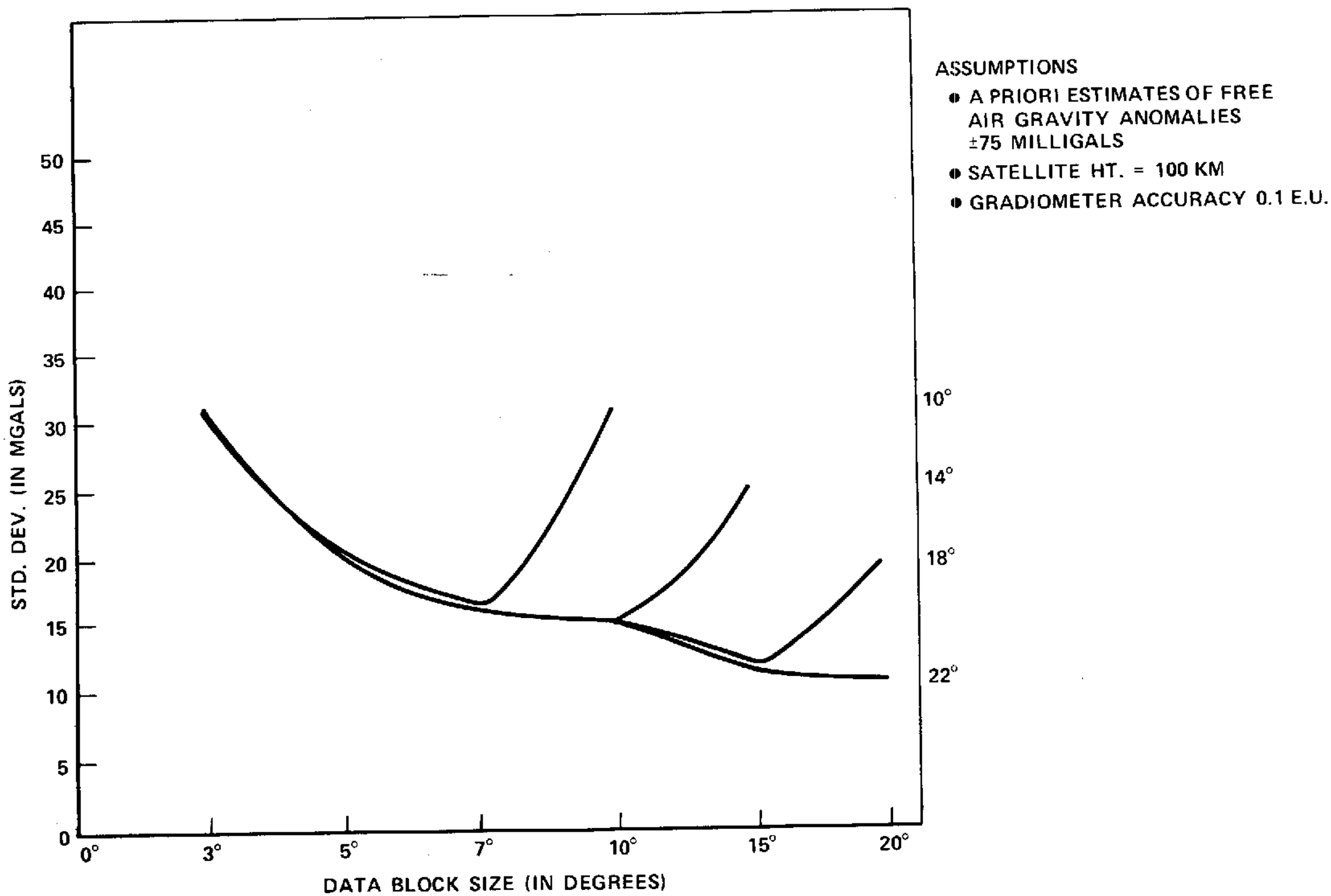

Figure 7. Accuracy of 2° by 2° Mean Free Air Gravity Anomaly Estimates vs. Data Block Size for Various Estimation Block Sizes

These results are dependent on the chosen value for the accuracy of the rotating gradiometer. Since this choice is somewhat arbitrary it is useful to parametrically represent gravity anomaly estimation accuracy as a function of gradiometer accuracy. Equation 18 implies that for a given choice of estimation block size and data block size, the standard deviation of a gravity anomaly estimate is the root sum square of a term which represents the aliasing effects of unadjusted gravity anomalies and a term which is proportional to the standard deviation of the rotating gradiometer observation. Assuming a 10° data block size and that a given gravity anomaly is simultaneously estimated with all gravity anomalies in the five adjacent layers, the estimation accuracy for 1° gravity anomalies at an altitude of 50 km is given as a function of data accuracy as

$$\sigma(1^\circ, 50\,\text{km}) = (12544\sigma^2 + 0.342)^{1/2} \tag{26a}$$

At the same altitude and for 5° data block size and for a buffer zone of rejected gravity anomaly estimates two deep, accuracies of estimates of 2° gravity anomalies are given as a function of data accuracy as

$$\sigma(2^\circ, 50\,\text{km}) = (9\sigma^2 + 0.36)^{1/2} \tag{26b}$$

At a height of 100 km and assuming a data block size of 20° and a buffer zone of rejected gravity anomalies five layers deep, the accuracies with which 2° gravity anomalies can be estimated are given as a function of data accuracy as

$$\sigma(2^\circ, 100\,\text{km}) = (16000\sigma^2 + 1)^{1/2} \tag{26c}$$

Standard deviations on the left side of the above equations are in mgal and the data standard deviation σ on the right side is in Etvos units.

CONCLUDING REMARKS

If a rotating gradiometer were placed on a satellite in a lunar polar orbit with an altitude in the 50 km to 100 km range, a dense and globally distributed set of gradiometer observations would be obtained in about 15 days. From this data set it should be possible to determine a global set of lunar gravity anomalies. But in order to keep the computational load within reasonable bounds it will be necessary to estimate local blocks of gravity anomalies in local blocks of gradiometer data. This report shows that if the satellite is flown at a 50 km altitude and if the proper estimation strategy is employed, an instrument with a .1E. accuracy permits estimates of 1° and 2° gravity anomalies which are accurate to within 12 mgal and 1 mgal. When the satellite is flown at 100 km, 2° gravity anomalies can be estimated with an accuracy of 12 mgal. Equation 26 of this report permit a scaling of these results to a data accuracy different from .1E.

REFERENCES

1. Heiskanen, W.A., and Morlty, H., Physical Geodesy, W.H. Freeman and Co., 1967

2. Argentiero, P., and Kahn, W., and Garza-Robles, R., Strategies For Estimating the Marine Geoid From Altimeter Data, NASA X-932-74-90, April 1974

3. Reed, George B., Application of Kinematical Geodesy for Determining the Short Wavelength Components of the Gravity Field by Satellite Gradiometry, The Ohio State University Research Foundation, Report No. 201, March 1973

4. Forward, R.L., Development of a Rotating Gravity Gradiometer For Earth Orbit Applications, Preprint and paper presented at the Advanced Applications Flight Experiment (AAFE) Program Review, 5-6 October 1971, NASA Research Center, Hampton, Va.